JOURNAL OF MATERIALS SCIENCE **35** (2000) 2009–2013

Optical constants and electrical conductivity of $Ge_{20}Se_{60}Sb_{20}$ thin films

A. A. ABU-SEHLY
Physics Department, Faculty of Science, Assiut University, Assiut, Egypt

Optical absorption and electrical resistivity of amorphous $Ge_{20}Se_{60}Sb_{20}$ films are investigated as a function of the thermal annealing. The dependence of the optical absorption coefficient on the photon energy is ascribed by the relation $(\alpha h\nu) = B(h\nu - E_o)^2$. Increasing the annealing temperature from 423 K to 553 K, decreases the optical gap of the film from 1.25 eV to 0.78 eV. The effect of annealing temperature on high frequency dielectric constant (ε_∞) and carrier concentration (N) was also studied. As a result of annealing the film at 533 K, the electrical resistivity and activation energy for conduction decreased from 5.7×10^7 to 2.9×10^2 $\Omega \cdot$cm and from 0.94 to 0.34 eV, respectively. The crystalline structures resulting from heat treatment at different elevated temperatures have been studied by X-ray Diffraction (XRD). The optical and electrical changes were attributed to the amorphous-crystalline transformations in the chalcogenide films.

1. Introduction

In recent years, optical memory effect in amorphous semiconductors films have been investigated and utilized for various application [1–3]. These have distinct advantages, viz., large packing density, mass replication, first data rate, high signal to noise ratio, and high immunity to defects [1–3]. Glassy chalcogenide semiconductors have great varieties of band gaps and are transparent in the IR region. The use of these films for reversible optical recording by the amorphous to crystalline phase change has recently been reported [4, 5]. The chalcogenides used for recording medium must be easy to amorphize and crystallize. There should be a high optical contrast between the amorphous and crystalline states. Furthermore, the writing and erasing must be fast and the material should be stable to an adequate number of write and erase cycles and have good oxidation resistance.

Thermal processes are known to be important in inducing crystallization in semiconducting chalcogenide glasses [6, 7]. Crystallization is associated with electrical changes which can reflect to a large extent the amount of converted in thermally annealed chalcogenide films [8–11]. Crystallization of chalcogenide films is accompanied by a decrease in the optical energy gap [12], as well as electrical resistivity [10]. Separation of different crystalline phases with thermal annealing was observed in ternary glasses [13]. The change in the optical energy gap could be determined by identification of the transformed phases. The reported results for the optical gap of pseudo binary systems indicated a monotonic decrease with increasing concentration of the low optical gap phase [13–15].

In the present work, a systematic study of the optical and electrical properties of the $Ge_{20}Se_{60}Sb_{20}$ amorphous thin films was made. The effect of thermal annealing on the optical energy gap (E_o), high frequency dielectric constant (ε_∞), carrier concentration (N) and the activation energy for conduction (ΔE) were studied. X-ray diffraction was used to determine the structural changes of $Ge_{20}Se_{60}Sb_{20}$ films under different annealing conditions.

2. Experimental details

Bulk $Ge_{20}Se_{60}Sb_{20}$ chalcogenide glass was prepared by the melt-quenching technique [13, 16]. Differential scanning calorimetry (DSC) was carried out using a Schimadzu TA-50 (Japan) instrument, at a heating rate of 25 K min^{-1}. Powder of the as-prepared and annealed specimens was examined using a Philips diffractometer type 1710 with Ni-filtered Cu K source ($\lambda = 0.154$ nm), at 40 kV and 30 mA, with scanning speed 3.5 deg/min.

Thin films were prepared by thermal evaporation at 10^{-6} Torr using an Edwards coating system E-306. Thin film were deposited onto glass substrates (with refractive index 1.51) held at room temperature. The evaporation rate as well as the film thickness were controlled using a quartz crystal monitor FTM5. The absorbance (A) and transmittance (T) were recorded at room temperature using a double-beam spectrophotometer (Shimadzu UV-2101combined with PC) in the wavelength range 300–900 nm. The electrical conductivity measurements were carried out for films with evaporated gold gap (2.0×10 nm) electrodes, using a conventional circuit involving a keithley 610C electrometer. The measurements were carried out during heating the specimen in the temperature range 300–420 K using a Tohr cryogenic cryostat.

3. Results

DSC thermogram was obtained for a powdered $Ge_{20}Se_{60}Sb_{20}$ glass sample of weight 16.4 mg using a heating rate of 25 K · min^{-1}. As shown in Fig. 1, the glass transition temperature and the peak temperature crystallization are 439.8 K and 529 K, respectively.

The effect of one hour annealing under constant flow of nitrogen gas at temperatures 448, 498 and 548 K on the X-ray diffraction pattern of the $Ge_{20}Se_{60}Sb_{20}$ films are shown in Fig. 2. According to A.S.T.M card [17,18], the identified crystalline phases are Sb_2Se_3, Ge_4Sb_6, $GeSe_2$ and GeSe.

3.1. Absorption edge

Study of the optical constant in the vicinity of the absorption edge have yielded significant information on the role of various atoms in the chalcogenide network. It is known that, if multiple reflections are neglected, the transmission T of a perfectly smooth film deposited on a perfectly smooth substrate can be determined by the following relation [19, 20].

$$T = (1 - R)^2 \exp(-A) = (1 - R)^2 \exp(-\alpha d) \quad (1)$$

where R is the reflectance, A the absorbance, α is the optical absorption coefficient in (cm^{-1}) and d is the film thickness.

Fig. 3, shows the effect of annealing temperature on the optical transmittance of the $Ge_{20}Se_{60}Sb_{20}$ thin films. It is easily seen that the films transparency decreases with increasing the annealing temperature. According to Tauc [21], in the high absorption region ($\alpha > 10^4$ cm^{-1}), the photon energy dependence of the absorption coefficient can be described by the following relation,

$$(\alpha h\nu) = B(h\nu - E_o)^r \quad (2)$$

where B is a parameter that depends on the transition probability, E_o is the characteristic energy of the transition, and r is an index which depends on the nature of the electronic transition responsible for the absorption [21].

The experimental results for the as-prepared $Ge_{20}Se_{60}Sb_{20}$ thin films at different thicknesses show a good fit to Equation 2 with $r = 2$. This result indicates that indirect transition is the most probable mechanism. The optical gap of the indirect transition can be obtained from the intercept of the $(\alpha h\nu)^{1/2}$ vs. $h\nu$ plots with the energy axis at $(\alpha h\nu)^{1/2} = 0$, as shown Fig. 4. The values of the indirect optical energy gap as a function of the annealing temperature of the films are shown in Fig. 5. It is observed that E_o slightly increases with increasing the annealing temperature up to 423 K, followed by a sharp decrease with increasing the annealing

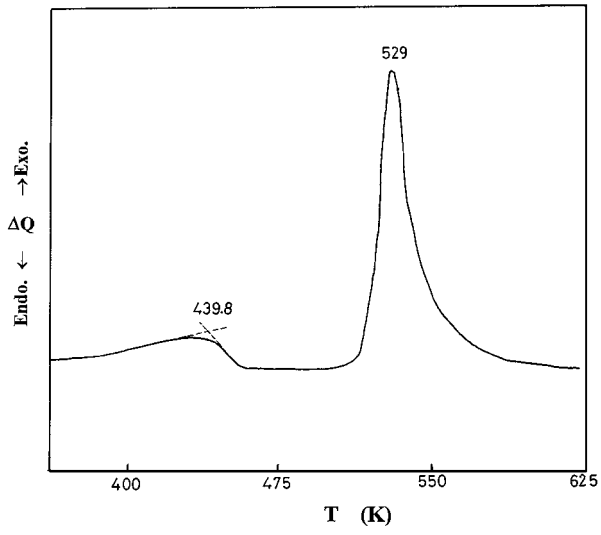

Figure 1 DSC trace for powdered $Ge_{20}Se_{60}Sb_{20}$ glass.

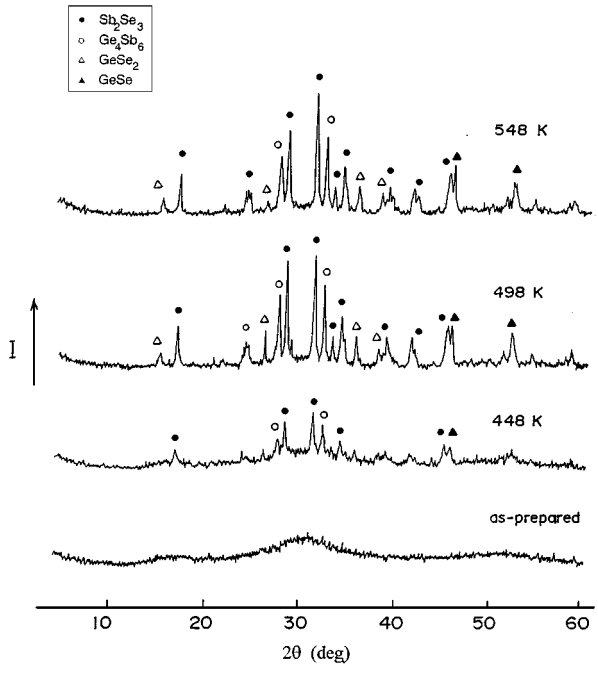

Figure 2 X-ray diffraction pattern for as prepared $Ge_{20}Se_{60}Sb_{20}$ film and annealed at 448, 498 and 548 K for 1.0 h.

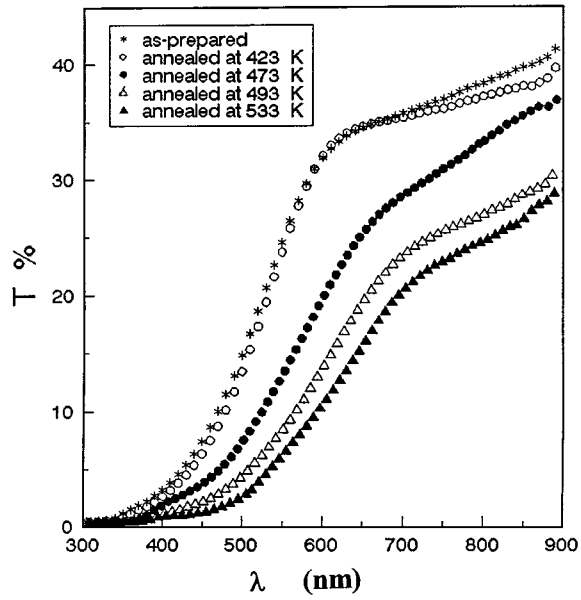

Figure 3 The spectral dependence of the transmittance for as-prepared and annealed $Ge_{20}Se_{60}Sb_{20}$ films.

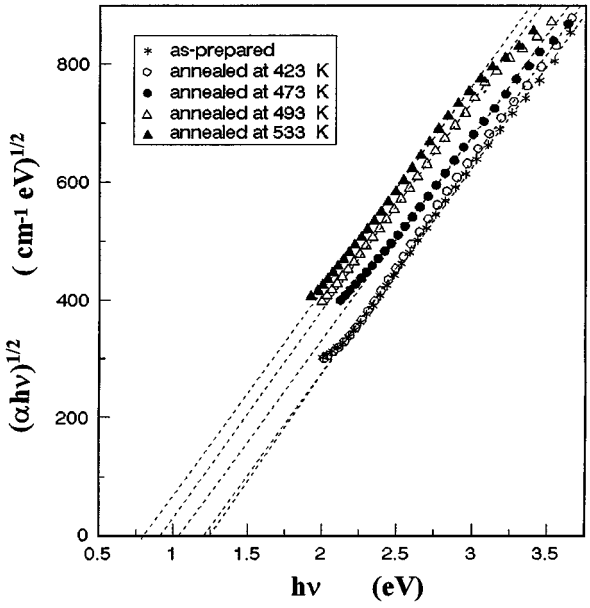

Figure 4 The absorption coefficient plotted as $(\alpha h\nu)^{1/2}$ vs. $h\nu$ for as-prepared and annealed $Ge_{20}Se_{60}Sb_{20}$ films.

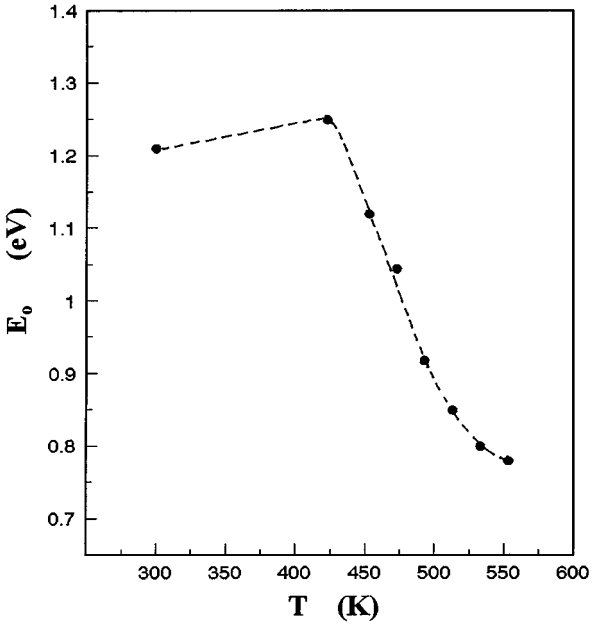

Figure 5 The effect of annealing temperature on the indirect optical energy gap (E_o) for $Ge_{20}Se_{60}Sb_{20}$ thin films.

temperature above the glass transition temperature. The effect of the annealing temperature on the values of E_o and B are given in Table I.

3.2. High frequency dielectric constant (ε_∞) and carrier density (N)

For a better understanding of the optical properties of the investigated film, it is necessary to determine some optical constants such as high frequency dielectric constant (ε_∞) and carrier concentration (N). Any absorbing medium can be characterized by the complex refractive index ($n - ik$) and complex dielectric constant ($\varepsilon_{\infty 1} - i\varepsilon_{\infty 2}$) where n and $k(\alpha\lambda/4\pi)$ are the real refractive index and extinction coefficient, respectively [20].

Reflectance of the film can be calculated from the experimentally measured values of the transmittance and absorbance using Equation 1. The refractive index of the film can be given [19] from the following relation,

$$R = \frac{[(n-1)^2 + k^2]}{[(n+1)^2 + k^2]} \tag{3}$$

Accordingly [20, 22, 23] the real component of the relative permittivity (ε') and the square of wavelength (λ^2) are related by the following equation:

$$\varepsilon' = n^2 = \varepsilon_\infty - \left(\frac{e^2}{\pi c^2}\right) \cdot \left(\frac{N}{m^*}\right)\lambda^2 \tag{4}$$

where n is the refractive index, e the electronic charge and c the velocity of light. For a linear plot of ε' vs λ^2, the high frequency dielectric constant (ε_∞) and the ratio N/m^* of the investigated film can be determined.

Fig. 6a, shows the relation between the refractive index (n) vs. λ. It is clear that the refractive index (n) decreases with increasing λ and the decrease becomes insignificant at long wavelength ($\lambda \geq 700$ nm). The nearly constant value of n at higher wavelength ($\lambda = 900$ nm) was termed as n_o and listed in Table I.

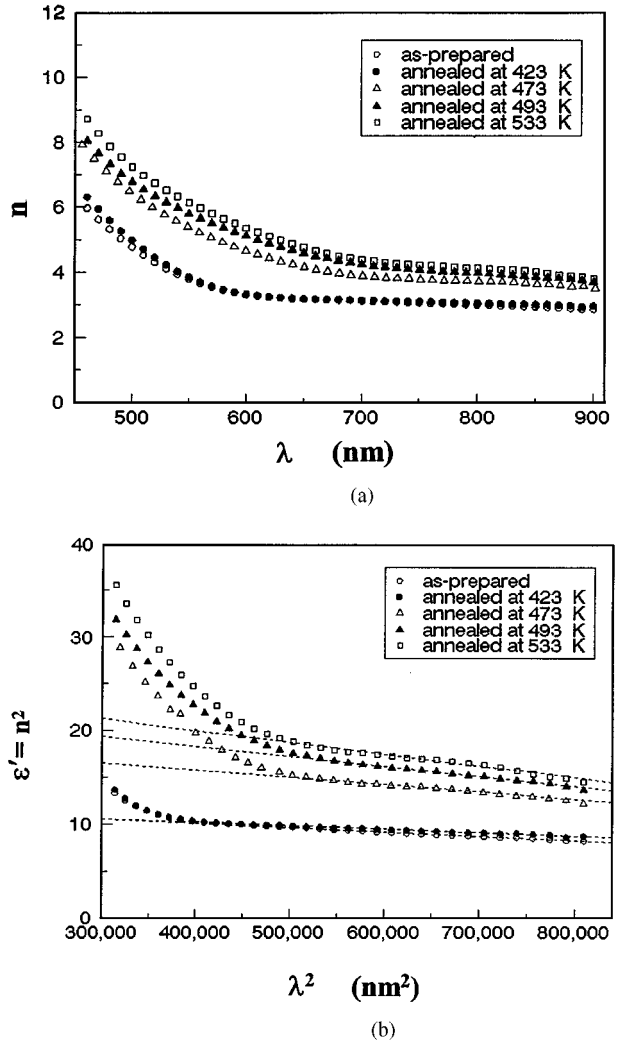

Figure 6 (a–b) Plot of the refractive index (n) and the relative permittivity (ε') vs λ for as-prepared and annealed $Ge_{20}Se_{60}Sb_{20}$ films.

TABLE I The dependence of the indirect optical energy gap E_o, constant B, the refractive index, the high frequency dielectric constant (ε_∞) and the ratio (N/m^*) on the annealing temperature of $Ge_{20}Se_{60}Sb_{20}$ films

Annealing temperature (K)	E_o (eV)	$B \times 10^5$ (cm^{-1} eV^{-1})	n_o	ε_∞	$N/m^* \times 10^{22}$ (cm^{-3})
300	1.21 ± 0.010	1.26	2.87	11.88 ± 0.04	0.45
423	1.25 ± 0.011	1.29	2.96	11.63 ± 0.03	0.34
453	1.12 ± 0.013	1.27	3.43	14.20 ± 0.05	0.55
473	1.05 ± 0.015	1.23	3.60	18.25 ± 0.04	0.78
493	0.92 ± 0.012	1.23	3.70	22.49 ± 0.07	1.12
513	0.85 ± 0.016	1.22	3.78	23.92 ± 0.07	1.25
533	0.80 ± 0.013	1.16	3.81	25.02 ± 0.09	1.34
553	0.78 ± 0.011	1.15	3.83	25.86 ± 0.10	1.40

Fig. 6b, shows the effect of temperature annealing on the ε' vs λ^2 plots. It could noticed that the relative permittivity (ε') decreases exponentially with increasing λ^2. To obtain the high frequency dielectric constant Equation 4 was applied, on the linear part of the relation between ε' versus λ^2. The intersection at $\lambda^2 = 0$ for the linear part of this curve at high wavelength gives the high frequency dielectric constant (ε_∞) and the slope gives the ratio N/m^*. It could noticed that, the high frequency dielectric constant (ε_∞) and the ratio N/m^* increase with increasing the annealing temperature. The effect of annealing temperature on the high frequency dielectric constant (ε_∞) and the ratio N/m^* are given in Table I.

Fig. 7a and b, shows the dependence of the real part of dielectric constant ($n^2 - k^2$) and the imaginary part of dielectric constant ($2nk$) on the photon wavelength (λ) after annealing at different temperature, respectively.

3.3. Electrical conduction

The effect of annealing temperature on the electrical resistivity of the as-prepared $Ge_{20}Se_{60}Sb_{20}$ films, 200 nm thick, was studied. Fig. 8, shows log ρ vs $1/T$ plots for the as-prepared and annealed films. The temperature dependence of the resistivity can be described using the relation

$$\rho = \rho_o \exp\left(\frac{\Delta E}{kT}\right) \tag{5}$$

where ΔE is the activation energy for conduction in eV, k is Boltzman constant and ρ_o is the resistivity pre-exponent factor. The value of the activation energy for conduction (ΔE) and the room temperature resistivity ($\rho_{R.T.}$), calculated from Fig. 8, are given in Table II.

TABLE II The activation energy (ΔE) for conduction and the room temperature resistivity ($\rho_{R.T.}$) for as-prepared and annealed $Ge_{20}Se_{60}Sb_{20}$ films

Annealing temperature (K)	ΔE (eV)	$\rho_{R.T.}$ ($\Omega \cdot cm$)
300	0.99 ± 0.020	5.70×10^7
453	0.94 ± 0.018	2.36×10^7
473	0.63 ± 0.012	4.68×10^5
493	0.51 ± 0.013	7.75×10^3
513	0.37 ± 0.010	7.26×10^2
533	0.34 ± 0.011	2.94×10^2

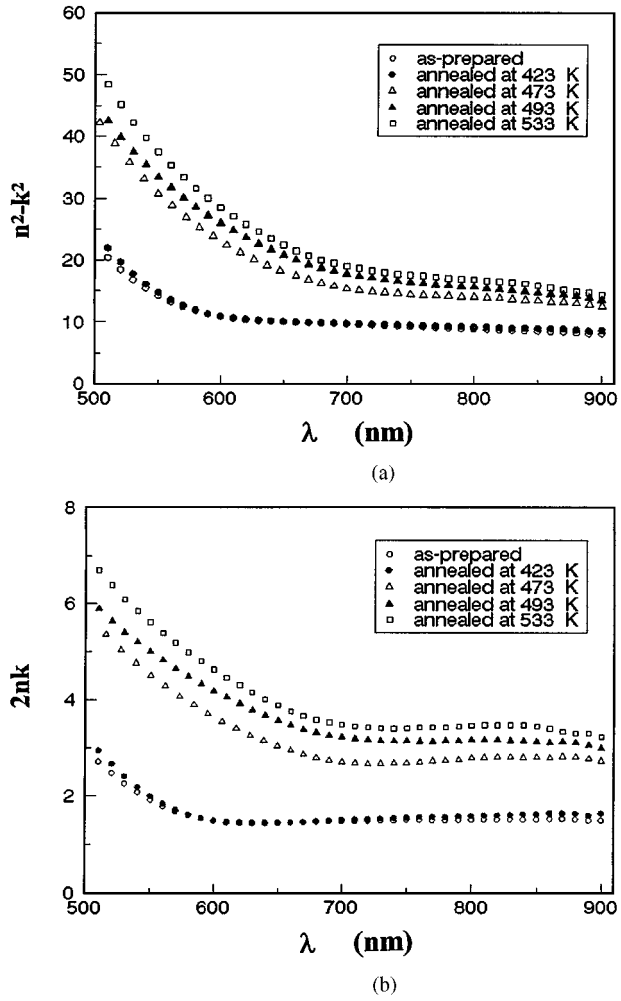

Figure 7 (a–b) Plot of the really part of dielectric constant ($n^2 - k^2$) and the imaginary part of dielectric constant ($2nk$) vs λ for as-prepared and annealed $Ge_{20}Se_{60}Sb_{20}$ films.

4. Discussion

The general features of the density of states of amorphous solids can be understood from the model proposed by Mott and Davis [24, 25]. During thermal annealing at temperatures below the glass transition temperature T_g, the unsaturated defects are gradually annealed out producing a larger number of saturated bonds [16, 26]. The reduction in the number of unsaturated defects decreases the density of localized states in the band structure [27], consequently increasing the optical gap (Fig. 5). Thermal annealing at temperature higher than T_g decreases E_o in the gap region

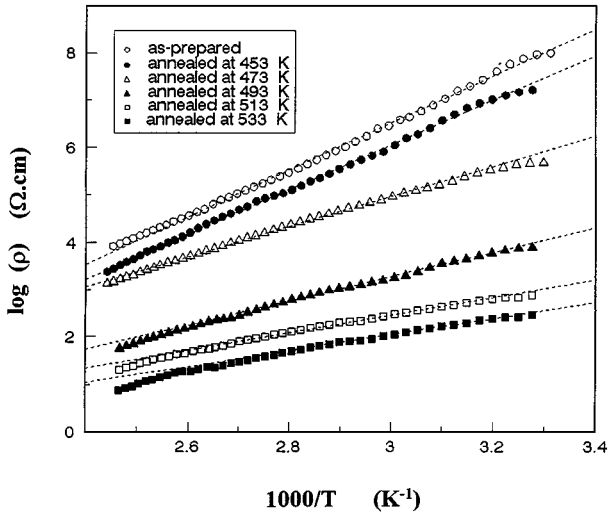

Figure 8 Plot of log ρ vs $1000/T$ for $Ge_{20}Se_{60}Sb_{20}$ thin films, as-prepared and annealed at different temperature for 1 h.

(Fig. 5). During annealing at temperature higher than T_g ($T_g = 439.8$ K), enough vibrational energy is present to break some of the weaker bonds, thus introducing some translational degrees of freedom to the system. The additional degrees of freedom result in an increase in the heat capacity. Crystallization via nucleation and growth becomes possible and depends on annealing temperature. XRD observations (Fig. 2) indicate amorphous-crystalline transformations for the annealed films. The continuous decrease in the indirect optical energy gap with increasing annealing temperature above 423 K could be attributed to the phase separation of crystalline phases (Fig. 2). The crystalline phase does not propagate homogeneously, and the mixture of amorphous are crystalline regions on a microscopic scale continues to change with annealing. Since the optical gap of crystalline Sb_2Se_3 is 0.70 eV [13, 28], the continuous decrease in the optical gap with increasing annealing temperature (Fig. 5), can be attributed to the increase in the amount of thermally crystalline Sb_2Se_3 [13, 16].

It could be noticed that the refractive index, dielectric constant and the ratio N/m^* increase with increasing the annealing temperature. It could be concluded that n_o (the refractive index at $\lambda = 900$ nm), ε_∞ and N/m^* are strongly dependent on the internal microstructure change induced by heat treatment [20].

With further annealing at temperatures $\geq$453 K the electrical resistivity and the activation energy decrease, as shown in Table II. Since the activation energy of crystalline $Sb_{20}Se_{80}$ is 0.35 eV [29], the continuous decrease in the activation energy with increasing annealing temperature can be attributed to the amorphous-crystalline transformations [13, 29].

5. Conclusions

The optical absorption measurements for $Ge_{20}Se_{60}Sb_{20}$ thin films indicate that the absorption mechanism is due to indirect transition. The optical energy gap (E_o) increases with increasing the annealing temperature up to the glass transition temperature T_g, followed by sharp decrease on increasing the annealing temperature above T_g. The optical parameters n_o, ε_∞ and N/m^* are affected by the film annealing temperature.

(XRD) showed that the amorphous-crystalline transformation occurred after annealing at temperature $>$423 K.

The electrical resistivity and the activation energy for conduction were found to decrease with increasing the annealing temperature.

Acknowledgements

The author thanks Dr. A.H. Moharram for his continuous encouragement and stimulating discussion.

References

1. ZISHAN H. KHAN, M. ZULFEQUAR, T. P. SHARMA and M. HUSAIN, *Optical Materials* **6** (1996) 139.
2. K. A. RUBIN and M. CHEN, *Thin Solid Films* **181** (1989) 129.
3. P. F. CARCIA, F. D. KALK, P. E. BIERSTEDT, A. FERRETTI, G. A. JONES and D. G. SWARIZFAGER, *J. Appl. Phys.* **64** (1988)1715.
4. D. P. GOSAIN, T. SHIMIZU, M. OHMURA, M. SUZUKI, T. BANDO and S. OKANO, *J. Mater. Sci.* **26** (1991) 3271.
5. R. M. MEHRA, R. KUMAR and P. C. MATHUR, *Thin Solid Films* **170** (1989) 15.
6. R. T. JOHNOS, JR. and R. K. QUINN, *J. Appl. Phys.* **43** (1972) 3875.
7. R. K. QUINN and R. T. JOHNOS, *J. Non-Cryst. Solids* **7** (1972) 53.
8. A. BIENENSTOCK, F. BETTS and S. R. OVSHINSKY, *ibid.* **2** (1970) 347.
9. S. C. MOSS and J. P. DENEUFVILLE, *ibid.* **8–9** (1972) 45.
10. M. M. HAFIZ, M. M. IBRAHIM, M. DONGOL and F. H. HAMMAD, *J. Appl. Phys.* **54** (1983) 1950.
11. A. H. MOHARRAM and M. S. RASHEEDY, *Phy. Sta. Sol. (a)* **169** (1998) 33.
12. M. DIGIULIO, D. MANNO, R. RELLA, P. SICILIANO and A. TEPORE, *Sol. Energy Mater.* **15** (1987) 209.
13. M. M. HAFIZ, A. H. MOHARRAM, M. A. ABDEL-RAHIM and A. A. ABU-SEHLY, *Thin Solid Films* **292** (1997) 7.
14. T. N. VENGEL and B. T. KOLOMIETS, *Sov. Phys. Tech. Phys.* **27** (1957) 2317.
15. J. P. DENEUFVILLE, *J. Non-Cryst. Solids* **8–10** (1972) 85.
16. M. M. HAFIZ, M. A. ABDEL-RAHIM and A. A. ABU-SEHLY, *Physica B* **252** (1998) 207.
17. CARRON, *Acta Crystallogr* **16** (1963) 338.
18. HONEA, *Am. Mineral.* **49** (1964) 325.
19. T. S. MOSS, "Semiconductor Opto-Electronics," (Butterworth & Co., London, 1973) p. 19.
20. E. KH. SHOKR and M. M. WAKKAD, *J. Mater. Sci.* **27** (1992) 1197.
21. J. TAUC, in "Amorphous and Liquid Semiconductors," edited by J. Tauc (Plenum, New York, 1974) Ch. 4.
22. W. G. SPITZER and H. Y. FAN, *Phys. Rev.* **166** (1957) 882.
23. M. M. WAKKAD, *J. Phys. Chem. Solids* **51** (1990) 1171.
24. N. F. MOTT, *Philos. Mag.* **19** (1969) 835.
25. N. F. MOTT and E. A. DAVIS, "Electronic Process in Non-Crystalline Materials," (Clarenden Oxford, 1979) Ch. 9.
26. S. HASEGAWA, S. YAZALCI and T. SHIMIZU, *Solid State Commun.* **26** (1978) 407.
27. A. S. MAAN, D. R. GOYAL, S. K. SHARMA and T. P. SHARMA, *J. Non-Cryst. Solids* **183** (1995) 186.
28. K. SHIMAKAWA, *J. Non-Cryst. Solids* **43** (1981) 229.
29. P. SIKKA and K. KUMAR, *J. Mater. Sci.* **29** (1992) 1781.

Received 3 September 1998
and accepted 30 September 1999